



Research Publication Repository

<http://publications.wehi.edu.au/search/SearchPublications>

This is the author's peer reviewed manuscript version of a work accepted for publication.

Publication details:	Janic A, Valente LJ, Wakefield MJ, Di Stefano L, Milla L, Wilcox S, Yang H, Tai L, Vandenberg CJ, Kueh AJ, Mizutani S, Brennan MS, Schenk RL, Lindqvist LM, Papenfuss AT, O'Connor L, Strasser A, Herold MJ. DNA repair processes are critical mediators of p53-dependent tumor suppression. <i>Nature Medicine</i> . 2018 24(7):947-953.
Published version is available at:	https://doi.org/10.1038/s41591-018-0043-5

Changes introduced as a result of publishing processes such as copy-editing and formatting may not be reflected in this manuscript.

Sensitised *in vivo* shRNA screens identify effectors of p53-mediated tumour suppression and reveal a critical role of DNA repair

Ana Janic^{1,2}, Liz J Valente^{1,2,3+}, Matthew J Wakefield^{1,4+}, Leon Di Stefano¹, Liz Milla^{1,2}, Stephen Wilcox^{1,2}, Haoyu Yang^{1,2,5}, Lin Tai¹, Cassandra J Vandenberg^{1,2}, Andrew J Kueh^{1,2}, Shinsuke Mizutani^{1,2}, Margs S Brennan^{1,2}, Robyn L Schenk^{1,2}, Lisa M Lindqvist^{1,2}, Anthony T Papenfuss^{1,2,6}, Liam O'Connor^{1,2*}, Andreas Strasser^{1,2*#}, Marco J Herold^{1,2*}

¹ The Walter and Eliza Hall Institute of Medical Research, Molecular Genetics of Cancer Division, 1G Royal Parade, Parkville, Melbourne, Victoria 3052, Australia

² Department of Medical Biology, University of Melbourne, Parkville, Melbourne, Victoria 3050, Australia

³ current address: Stanford University School of Medicine, Division of Radiation Oncology-Radiation and Cancer Biology, Stanford, California, 94305, USA

⁴ Melbourne Bioinformatics, The University of Melbourne, Carlton, VIC 3053, Australia

⁵ School of Pharmaceutical Sciences, Tsinghua University, Beijing, 100084, China

⁶ Peter MacCallum Cancer Centre, Parkville, VIC 3052, Australia

+ these authors contributed equally to this work

* these authors share senior authorship

corresponding author:

Andreas Strasser

The Walter and Eliza Hall Institute

1G Royal Parade

Parkville, VIC 3052

Australia

Phone: +61-3-9345-2624

FAX: +61-3-9347-0852

Email: strasser@wehi.edu.au

Summary

It has long been assumed that p53 suppresses tumour development through induction of apoptosis, possibly with contributions by cell cycle arrest and cell senescence^{1,2}. However, combined deficiency in these three processes, unlike loss of p53, does not cause spontaneous tumour development, relaunching the search for the mechanisms that are critical for p53 to suppresses tumorigenesis³⁻⁵. To define such mechanisms, we performed sensitised *in vivo* screens in mice with an shRNA library targeting p53-regulated genes. We found that knockdown of three of the hits, *Zmat3*, *Ctsf* and *Cav1*, promoted lymphoma/leukaemia development only when PUMA and p21, the critical effectors of p53-driven apoptosis, cell cycle arrest and senescence, were also absent. Notably, loss of the DNA repair gene *Mlh1*, caused lymphoma in a wild-type background and its enforced expression was able to delay tumour development driven by loss of p53. Knockdown of *Mlh1*, *Msh2*, *Rnf144b*, *Cav1* and *Ddit4*, all direct p53 target genes and implicated in DNA repair, accelerated MYC-driven lymphoma development to a similar extent as knockdown of p53. Collectively, these findings demonstrate that extensive functional overlap of several p53-regulated processes safeguards against cancer and that, at least within the haematopoietic compartment, coordination of DNA repair appears to be an important process by which p53 suppresses tumour development.

The tumour suppressor gene *p53* is mutated in ~50% of human cancers⁶. In addition to its critical role in preventing tumour development, *p53* also constitutes a major determinant of the cellular response to genotoxic cancer therapy^{1,7,8}. Accordingly, mice lacking functional *p53* are highly predisposed to developing cancer and their cells are resistant to genotoxic anti-cancer agents^{9,10}. As a transcription factor *p53* regulates expression of ~300 target genes to coordinate diverse cellular effector functions, including apoptotic cell death, cell cycle arrest and cellular senescence^{11,12}. Although these processes were widely thought to be essential for *p53*-mediated tumour suppression^{1,7}, surprisingly, no tumours arose in mice lacking PUMA, NOXA and *p21*⁵, the critical mediators of *p53*-induced apoptosis^{13,14} and G1/S cell cycle arrest/cell senescence¹⁵, respectively, or in mice bearing mutations in *p53* that impair transcriptional activation of these genes^{3,4}. Moreover, loss of even a single *p53* allele accelerated c-MYC-driven lymphomagenesis to a much greater extent than complete loss of either PUMA and NOXA or PUMA and *p21*^{16,17}. Thus, *p53* must suppress tumour development through currently underappreciated processes that either overlap with, or are distinct from induction of apoptosis, cell cycle arrest and cell senescence.

To define the mechanisms critical for *p53*-mediated tumour suppression we conducted *in vivo* screens using a pooled shRNA library containing 930 shRNAs targeting 166 known *p53* target genes (5-6 shRNAs per gene) compiled from published gene expression and CHIP-sequencing data (Fig. 1a, Supplementary Table 1)^{3,18}. The first screen was sensitised by the absence of the critical effectors of *p53*-driven apoptosis, cell cycle arrest and senescence (*Puma*^{-/-};*p21*^{-/-})⁵. When haematopoietic stem/progenitor cells (HSPCs) from foetal livers of E13.5 *Puma*^{-/-};*p21*^{-/-} or wt (C57BL/6-Ly5.2) embryos were transduced with a *p53* targeting shRNA and then transplanted into lethally irradiated wt (C57BL/6-Ly5.1) mice, 100% of recipients developed lymphoma/leukaemia within 300 days (Fig. 1b and Supplementary Fig. 1). Conversely, mice transplanted with *Puma*^{-/-};*p21*^{-/-} or wt HSPCs that had been transduced with an empty vector or a control shRNA targeting Renilla luciferase did not develop tumours (Fig. 1b and Supplementary Fig. 1). This establishes that our screening strategy was effective and had a low false positive rate.

Mice reconstituted with *Puma*^{-/-};*p21*^{-/-} HSPCs that had been transduced with the pooled *p53* target gene shRNA library developed lymphoma/leukaemia at an incidence of ~30% (21/67) within one

year (Fig. 1b). Genomic DNA was isolated from these tumours and the enriched shRNAs identified by amplicon sequencing. Most tumours contained several distinct shRNAs and, predictably, the *p53.848* shRNA was enriched in 4 of 27 tumours (Fig. 1c,d).

A complementary screen was conducted to search for shRNAs that could further accelerate c-MYC-driven lymphomagenesis even when p53-driven PUMA-mediated apoptosis is blocked. Mice reconstituted with *Eμ-Myc;Puma^{-/-}* HSPCs that had been transduced with the shRNA library developed lymphoma at an accelerated rate compared to mice reconstituted with control vector transduced *Eμ-Myc;Puma^{-/-}* HSPCs, although the *p53* shRNA (positive control) caused even greater acceleration (Fig. 1e). Lymphomas that arose in this shRNA library screen prior to 50 days post-transplantation were deemed accelerated and selected for genomic DNA analysis to identify the enriched shRNAs. The ‘hits’ from the two screens were ranked according to: (1) shRNAs that had highest enrichment in tumours, (2) number of tumours in which a particular shRNA was enriched, (3) independent shRNAs targeting the same gene found enriched in tumours (Fig. 1c,d,f,g and Supplementary Table 2,3).

Based on these criteria we selected fourteen genes for validation and shRNAs targeting each of these genes were introduced individually into *Puma^{-/-};p21^{-/-}* or *Eμ-Myc;Puma^{-/-}* HSPCs to test their ability to promote tumorigenesis in reconstituted animals. In the *Puma^{-/-};p21^{-/-}* HSPCs, knockdown of six of the fourteen genes tested (*Mlh1*, *Cav1*, *Zmat3*, *Ctsf*, *Rfwd2* and *Rb1*) caused leukaemia/lymphoma (mostly of myeloid origin, Supplementary Fig. 2a,b) in a significant fraction (10-75%) of reconstituted mice within a year (Fig. 2a and Supplementary Fig. 3a-c). In contrast, shRNAs targeting *Apc*, *Serpin1*, *Tl3*, *Ercc5*, *Ppm1j*, *Crip2*, *Tgfα*, *lincRNA-p21* did not promote tumorigenesis in this setting (Supplementary Fig. 3a). Therefore, these hits were not pursued. Notably, several independent shRNAs targeting *Mlh1* or *Cav1* accelerated lymphoma development in the *Eμ-Myc;Puma^{-/-}* background to a similar extent as p53 knockdown itself, whereas shRNAs targeting *Zmat3* or *Ctsf* had no impact (Fig. 2b and Supplementary Fig. 4a,b). This indicates that the importance of ZMAT3 and CTSF in p53-mediated tumour suppression may vary depending on the nature of the cooperating oncogenic lesions.

Western blot and qRT-PCRs analyses verified that the shRNAs targeting *Mlh1*, *Cav1*, *Zmat3*, *Ctsf*, *TGFα*, *Ercc5* and *Crip2* caused a reduction in the corresponding proteins and mRNAs,

respectively (Supplementary Fig. 5a-d). Moreover, qRT-PCR analysis and Western blotting confirmed that these now validated tumour suppressors were upregulated in thymocytes in a p53-dependent manner in response to γ -radiation or treatment with the MDM2 inhibitor nutlin-3a (Supplementary Fig. 6a,b). Knockdown of *Mlh1*, *Cav1*, *Zmat3* or *Ctsf* in *p53*^{-/-} HSPCs did not accelerate lymphoma development in reconstituted mice (Fig. 2c). This is consistent with the notion that these genes function in tumour suppression largely downstream of p53 rather than in parallel pathways.

Pathway analysis demonstrated that many validated hits from our screens function in DNA repair and cell division (Supplementary Table 4). Therefore and because of the potent impact of their knockdown on tumour development in the *Puma*^{-/-};*p21*^{-/-} and/or *E μ -Myc*;*Puma*^{-/-} backgrounds, we next focused on *Mlh1*, *Cav1* and *Zmat3*. First, we tested the published functions of *Cav1* and *Mlh1* in DNA repair^{19,20} and for *Cav1* we also assessed cell proliferation²¹. The comet assay revealed that pre-leukaemic *E μ -Myc*;*Puma*^{-/-} B lymphoid cells expressing shRNAs that target *Mlh1*, *Cav1* or *p53* (positive control) had more DNA lesions compared to control vector transduced cells (Supplementary Fig. 7a,b). DAPI staining showed that *Cav1* knockdown also significantly enhanced cycling of pre-leukaemic *E μ -Myc*;*Puma*^{-/-} B lymphoid cells (Supplementary Fig. 7c). *Zmat3* was reported to regulate cell death and cell proliferation²². To explore the function of *Zmat3* we used CRISPR/CAS9 technology to generate mutant mice lacking this protein (Supplementary Fig. 8a-e). Our examination of the ZMAT3-deficient animals showed that, unlike loss of p53, loss of ZMAT3 did not affect proliferation and apoptosis in lymphoid cells or cellular senescence in mouse embryonic fibroblast (Supplementary Fig. 9a-d). Collectively, these findings reveal that loss of MLH1 drives tumorigenesis exclusively through a direct defect in DNA repair whereas loss of CAV1 may increase DNA lesions by deregulating cell cycling.

For a highly critical effector of p53-mediated tumour suppression it would be expected that its loss could drive tumorigenesis on its own, i.e. on a wt background. Knockdown of *Cav1*, *Zmat3* or *Ctsf* did not cause leukaemia/lymphoma development in this setting (Fig. 3a). This reveals that their loss can only promote tumour development when p53-mediated apoptosis (via PUMA) and p53-mediated G1/S cell cycle arrest/senescence (via p21) are also impaired, demonstrating the extensive backup of multiple p53-regulated effector processes in tumour suppression. In contrast,

Mlh1 knockdown was able to cause lymphoma/leukaemia development on a wt background (Fig. 3a) and accelerated tumorigenesis on the *Eμ-Myc* background at a rate comparable to knockdown of *p53* itself (Fig. 3b). This indicates that MLH1 is a critical contributor to p53-mediated tumour suppression. Notably, in humans germ-line or acquired mutations in *Mlh1* cause non-polyposis colorectal cancer²³ and are responsible for a fraction of Li-Fraumeni Syndrome (LFS) patients who do not carry mutations in *p53*^{24,25}.

Tumours with defects in *p53* or genes implicated in DNA repair, such as *Mlh1*, usually present with extensive genomic abnormalities²⁶⁻²⁸. These aberrations might include nucleotide-level changes like single nucleotide variants (SNVs) and microsatellite instability, or structural variants, such as large-scale chromosome rearrangements and more focal gene amplifications or deletions. Using whole cancer genome sequencing, we observed a number of large-scale copy number changes in lymphomas driven by the *p53* shRNA, but comparatively fewer in those driven by the *Mlh1* shRNA and in control lymphomas (Fig. 3c, Supplementary Fig.10). Examining non-recurrent SNVs revealed a marked bias toward T>G/A>C substitutions in a subset of trinucleotide contexts (Supplementary Fig. 11a,b). There were no apparent differences in the numbers of substitutions observed across the tumours. However, short tandem repeat variants, an indicator of microsatellite instability, were markedly more numerous in lymphomas driven by *Mlh1* knockdown than among the other lymphomas (Fig. 3d, Supplementary Fig. 12). Control tumours showed a low number of structural and short tandem repeat genomic aberrations in these comparisons despite the longer (87 days vs ~40 days) tumour latency. These data are consistent with the notion that defects in MLH1-mediated DNA repair contribute to microsatellite instability, whereas tumours driven by loss of *p53* exhibit a broader pattern of genomic lesions.

Next, we tested the impact of enforced MLH1 expression on tumour development driven by loss of *p53*, either alone or in context of MYC over-expression. Of note, mice reconstituted with *Cas9* or *Eμ-Myc/Cas9* HSPCs that had been transduced with a vector encoding MLH1 and a *p53* sgRNA developed lymphoma at a slower rate compared to control mice reconstituted with HSPCs that had been transduced with vectors that encode only the *p53* sgRNA or a mutant of MLH1 that lacks its nuclear localisation sequence plus the *p53* sgRNA (Fig. 3e, Supplementary Fig. 13). These findings and those from the lymphoma genome analysis are consistent with the notion that loss of

p53 causes a reduction in the expression of not only *Mlh1* but of several DNA repair genes, with the loss of any of them potentially driving tumorigenesis. To test this hypothesis, we examined the roles of several DNA repair genes that are reportedly regulated by p53 - *Fancc*, *Polk*, *Ercc5*, *Pms2*, *Mgmt*, *Msh2*, *Rnf144b* and *Ddit4* - in tumour suppression (Supplementary Fig. 14a; Supplementary Table 4). Mice reconstituted with *Eμ-Myc* HSPCs that had been transduced with shRNAs targeting *Polk*, *Pms2* or *Mgmt* showed only a minor or no acceleration of lymphoma development compared to animals reconstituted with control *Eμ-Myc* HSPCs (Fig. 4a). Although these shRNAs potentially knocked down the mRNA and protein levels of their targets (Supplementary Fig. 14b-d), it cannot be excluded that even greater loss of these proteins would have accelerated tumorigenesis more substantially. Remarkably, knockdown of *Msh2*, *Rnf144b*, *Ddit4* or *Cav1* accelerated lymphoma development at a rate comparable to knockdown of *p53* itself, and knockdown of *Fancc* and *Ercc5* also enhanced lymphomagenesis, albeit to a lesser extent (Fig. 4a). Since some of these now validated tumour suppressor genes have been reported to regulate not only DNA repair but also several other processes, including cell proliferation or cell death (Supplementary Table 4), we tested their functions in pre-leukaemic *Eμ-Myc* B lymphoid cells (Supplementary Fig. 15a). In agreement with their published roles in DNA repair, comet assays validated that knockdown of these genes significantly increased DNA lesions in these cells (Supplementary Fig. 15b). Knockdown of *Cav1*, *Rnf144b* and *Ddit4*, but not knockdown of *Mlh1* or *Msh2*, also significantly enhanced the cycling of pre-leukaemic *Eμ-Myc* B lymphoid cells (Supplementary Fig. 7a, 15c), but none of the shRNAs impacted on apoptosis triggered by diverse cytotoxic insults (Supplementary Fig. 16 a-e). *Ddit4* was reported to act as a negative regulator of the mTORC1 pathway²⁹. However, Western blot analysis showed that knockdown of *Ddit4* did not perturb mTORC1 signaling in pre-leukaemic *Eμ-Myc* B lymphoid cells (Supplementary Fig. 17). Collectively, these findings are consistent with the notion that MLH1 and MSH2 exclusively function in DNA repair, whereas the ability of RNF144b, CAV1 and DDIT4 to restrain cell proliferation may suggest that they enable DNA repair by controlling cell cycling and thereby suppress tumorigenesis³⁰.

Whole genome sequencing analysis revealed that genomic aberrations in the lymphomas accelerated by the knockdown of *Rnf144b*, *Cav1*, *Ddit4*, and *Mlh1* were less extensive and abundant than those seen in lymphomas accelerated by knockdown of p53, which presented with large chromosome arm scale genomic lesions (Fig. 3c,4b and Supplementary Fig. 10,18a-b). These

findings are consistent with the notion that p53 maintains genome stability by orchestrating a broad array of DNA damage repair mechanisms³⁰. To provide evidence that p53 activated DNA repair processes are also critical for its tumour suppression in human cancers, we assessed whether mutations in DNA damage repair genes are mutually exclusive with mutations in p53. We found, indeed, that mutations in *Mlh1*, *Msh2*, *Rnf144b*, *Fancc*, *Cav1* and *Pms2* are mutually exclusive with mutations p53 within haematological cancers (Supplementary Fig. 19a,b). We expanded our analysis to colorectal cancer samples because they contain high rates of mutations in *p53* and strong DNA mismatch repair mutational signatures. We found that in these cancers not only mutations in the DNA mismatch repair genes *Mlh1*, *Msh2* or *Pms2*, but also mutations in *FancC* and *Rnf144b* are significantly mutually exclusive with mutations in *p53* (Fig. 4c, Supplementary Fig. 20a,b).

In conclusion, our work shows that *in vivo* shRNA screening in sensitised genetic backgrounds is a feasible approach to identify tumour suppressors. Our validation and functional assays indicate that p53 is a highly potent tumour suppressor because it can activate several tumour suppressive processes that cooperate and overlap to provide effective safeguard against cancer development (Fig. 4b). Thus, several p53-regulated processes must fail simultaneously for tumours to develop, for example loss of PUMA mediated apoptosis plus p21-mediated cell cycle arrest/senescence plus the process reliant on *Zmat3*. The relative importance of the different p53-activated cellular responses and the nature of their functional overlap in tumour suppression are likely to vary between different cell types and also in relation to the nature of the oncogenic drivers activated in the nascent neoplastic cells. Regardless, our findings suggest that coordination of DNA repair is a highly critical component of p53-mediated tumour suppression, at least within the context of hematological malignancies, consistent with the concept that p53 functions as the guardian of the genome²⁷.

Figure 1

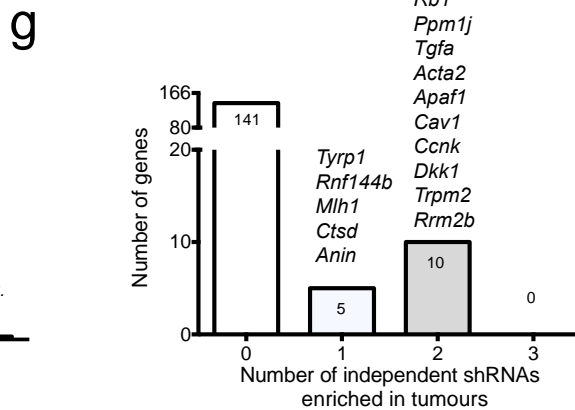
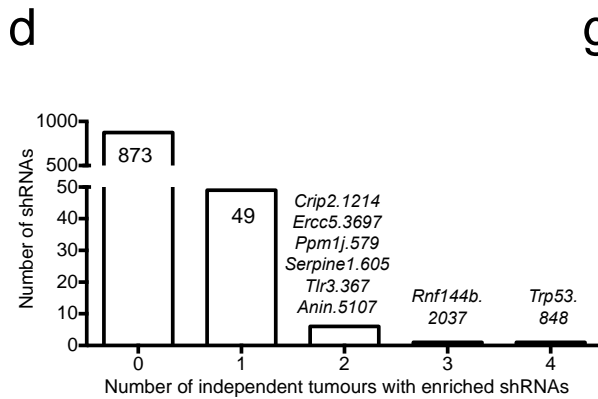
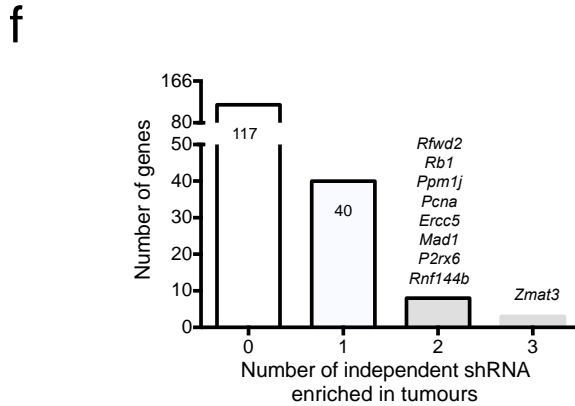
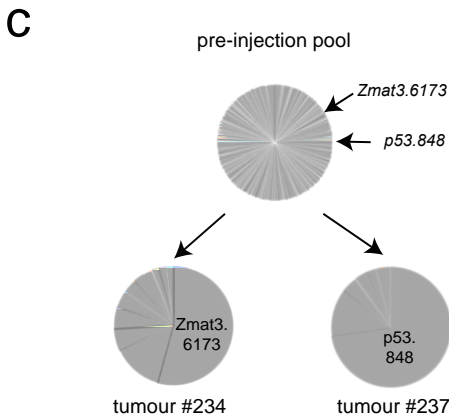
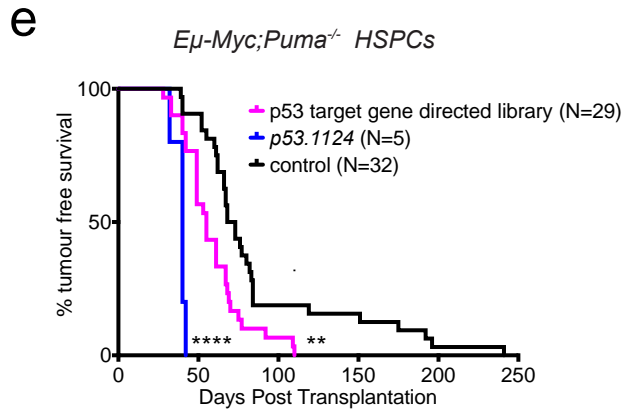
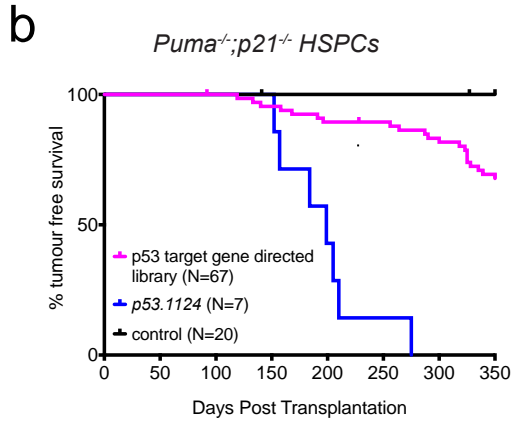
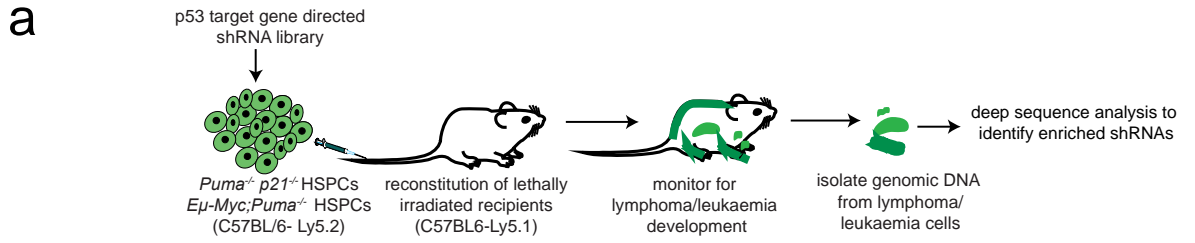
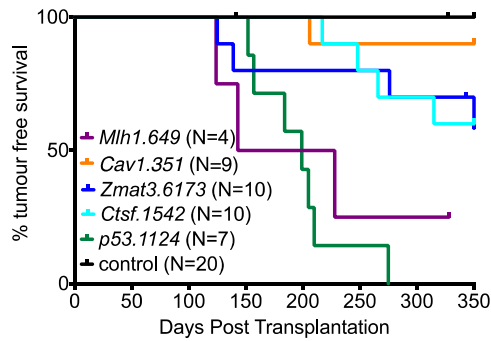


Figure 1 ***In vivo* shRNA library screening to identify critical effectors of p53-mediated tumour suppression.** **a** Experimental strategy of the screens. **b** Kaplan-Meier curve showing tumour-free survival of mice reconstituted with *Puma*^{-/-};*p21*^{-/-} HSPCs that had been transduced with vectors encoding shRNAs targeting *p53* (*p53.1124*; positive control), Renilla Luciferase, an empty vector (negative controls) or the p53 target gene directed shRNA library. N represents total number of reconstituted mice within a cohort. **c** Representative pie charts showing the fraction of total reads of a particular shRNA within the pre-injection pool or within individual tumours. **d** Number of tumours containing a particular enriched shRNA. A full list of the shRNAs enriched in these tumours is shown in Supplementary Table 2. **e** Kaplan-Meier curve showing tumour-free survival of mice reconstituted with *Em-Myc*;*Puma*^{-/-} HSPCs that had been transduced with an empty vector (negative control), the *p53.1124* shRNA (positive control) or the p53 target gene directed shRNA library. N represents total number of mice within a cohort. Median survival for control = 71 days post-transplantation; median survival for *p53.1124* shRNA = 40 days post-transplantation (compared to control, ***p<0.0001); median survival for p53 target gene directed shRNA library = 55 days post-transplantation (compared to control, **p=0.0012). **f** Number of genes with 0, 1, 2 or 3 shRNAs found enriched in the tumours. A full list of the genes for which shRNAs were found enriched in tumours is shown in Supplementary Table 3. **g** Number of genes with 0, 1, 2, and 3 independent shRNAs targeting that gene found in lymphomas arising within <50 days post-transplantation.

Figure 2

a

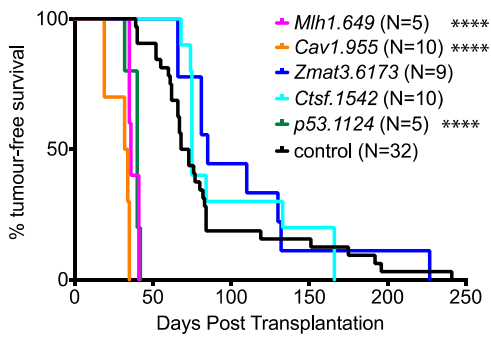
Puma^{-/-};*p21*^{-/-} HSPCs



gene	<i>Cav1</i>			<i>Mlh1</i>		<i>Zmat3</i>	<i>Ctsf</i>	<i>Rfwd2</i>	<i>Rb1</i>	<i>Tgfα</i>		<i>Crip2</i>		<i>Ercc5</i>		<i>Ppm1j</i>		<i>Apc</i>	<i>Serpine1</i>	<i>Ti3</i>	<i>lincRNA-p21</i>	
shRNA	955	351	2347	648	649	6173	1542	4896	580	4195	4061	718	1214	1711	3697	579	842	9841	605	367	172	
scored with tumour	+	+	+	+	+	+	+	+	+	-	+	-	+	-	-	-	-	-	-	-	-	-

b

Eμ-Myc;*Puma*^{-/-} HSPCs



gene	<i>Cav1</i>			<i>Mlh1</i>		<i>Zmat3</i>	<i>Ctsf</i>	<i>Rfwd2</i>	<i>Tgfα</i>		<i>Crip2</i>		<i>Ercc5</i>	
shRNA	955	351	2347	648	649	6173	1542	4896	4195	4061	718	1214	1711	3697
significantly accelerates tumorigenesis	+	+	+	+	+	-	-	-	-	-	-	-	-	-

c

p53^{-/-} HSPCs

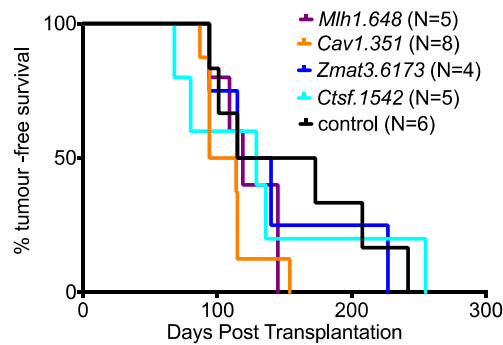


Figure 2 Validation of candidate tumour suppressors. a Kaplan-Meier curves showing tumour-free survival of mice reconstituted with *Puma*^{-/-};*p21*^{-/-} HSPCs that had been transduced individually with the indicated shRNAs. Table represents validation of the top shRNAs. **b** Kaplan-Meier curves showing tumour-free survival of mice reconstituted with *Eμ-Myc*;*Puma*^{-/-} HSPCs

that had been transduced individually with the indicated shRNAs. Median survival for control = 71 days, *p53.1124* shRNA = 40 days, *Cav1.955* shRNA = 33 days, *Mlh1.649* shRNA = 36 days, *Zmat3.6173* shRNA = 85 days, *Ctsf.1542* shRNA = 75 days post-transplantation (*Mlh1.649*, *Cav1.351* and *p53.1124* shRNA compared to control, all **** $p < 0.0001$). Table represents validation of the top shRNAs. Survival curves for mice reconstituted with *E μ -Myc;Puma^{-/-}* HSPCs transduced with a control shRNA vector (negative control) and *p53* shRNA (positive control) constitute the aggregate from several independent experiments and they are also shown as controls in Fig. 1e and Supplementary Fig. 4a,b. c Kaplan-Meier curves showing tumour-free survival of mice reconstituted with *p53^{-/-}* HSPCs that had been transduced individually with the indicated shRNAs. Median survival for control = 144 days, *Cav1.955* shRNA = 104 days, *Mlh1.648* shRNA = 119 days, *Zmat3.6173* shRNA = 128 days, *Ctsf.1542* shRNA = 129 days post-transplantation. N represents total number of reconstituted mice within a cohort.

Figure 3

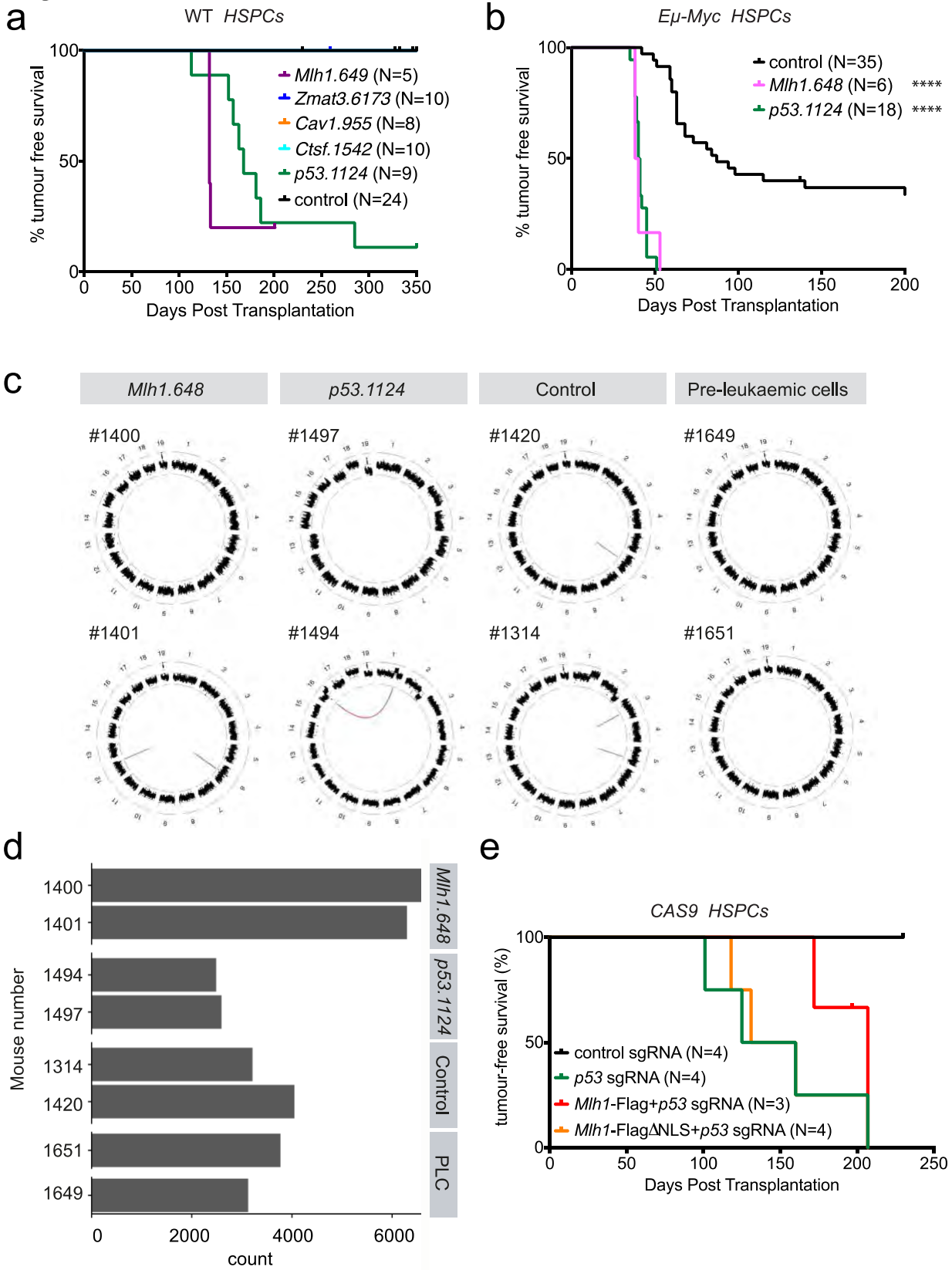
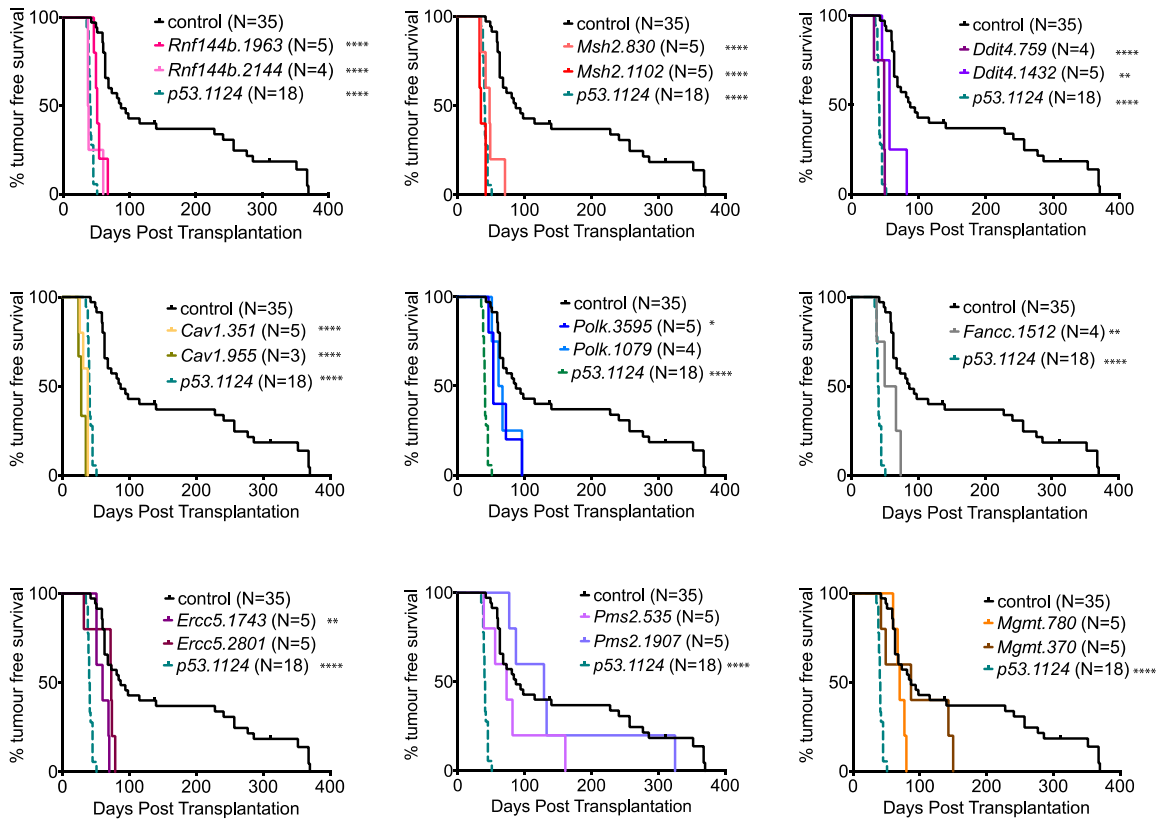


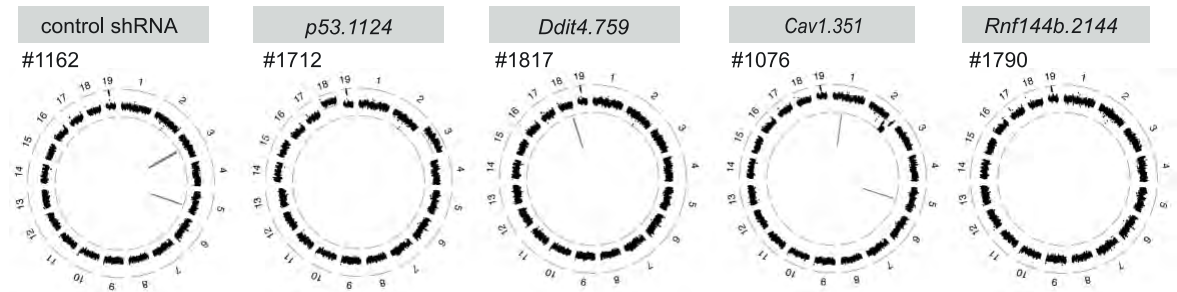
Figure 3 **MLH1 is a potent tumour suppressor.** **a** Kaplan-Meier curves showing tumour-free survival of mice reconstituted with wt HSPCs that had been transduced with the indicated shRNAs. **b** Kaplan-Meier curves showing tumour-free survival of mice reconstituted with *Eμ-Myc* HSPCs that had been transduced with the indicated shRNAs. Median survival for control = 87 days, for *p53.1124* = 41 days, for *Mlh1.648* = 39 days post-transplantation (compared to control, **** $p < 0.0001$). **c** CIRCOS plots of log₂ fold-change in copy number (black dots), inter-chromosomal translocations (red lines) and intra-chromosomal structural variants (blue lines). *Eμ-Myc* lymphomas accelerated by an shRNA against *Mlh1* (#1400 and #1401), by an shRNA against *p53* (#1494 and #1497), and control *Eμ-Myc* lymphomas (#1314 and #1420, transduced with an empty vector or a vector encoding an shRNA targeting Renilla luciferase); #1651 pre-leukaemic *Eμ-Myc* B lymphoid cells transduced with shRNAs against *Mlh1*, and #1649 non-transduced (control) pre-leukaemic *Eμ-Myc* B lymphoid cells. **d** Short Tandem Repeat (STR) variants in the lymphoma and pre-leukaemic cells (PLC). The differences consist mostly in single-nucleotide reductions in motif length (Supplementary Fig. 12). **e** Kaplan-Meier curve showing tumour-free survival of mice reconstituted with HSPCs expressing CAS9 that had been transduced with the following vectors: human *Bim* sgRNA (negative control), *p53* sgRNA (positive control), *p53* sgRNA plus wild-type *Mlh1*-Flag, *p53* sgRNA plus *Mlh1*-FlagΔNLS (mutant of MLH1 lacking its nuclear localisation sequence). Median survival for *p53* sgRNA = 142 days, *Mlh1*-FlagΔNLS + *p53* sgRNA = 145 days, wild-type *Mlh1*-Flag + *p53* sgRNA = 207 days. N represents total number of reconstituted mice within a cohort.

Figure 4

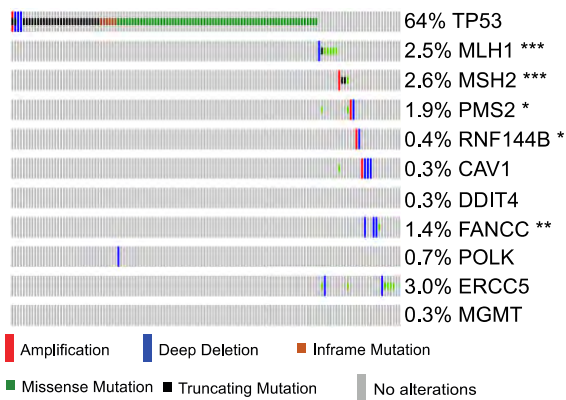
a



b



c



d

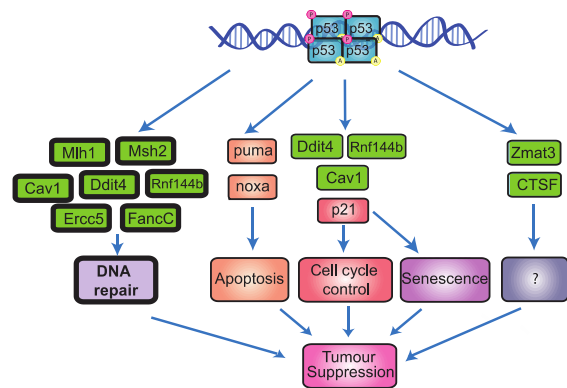


Figure 4 Several p53-regulated DNA repair genes function as tumour suppressors.

a Kaplan-Meier curves showing tumour-free survival of mice reconstituted with *Eμ-Myc* HSPCs that had been transduced with the indicated shRNAs. Median survival post-transplantation: control = 87 days, for *p53.1124* = 41 (positive control) for *Rnf144b.2144* = 38 and *Rnf144b.1963* = 51 days (**** $p < 0.0001$), for *Msh2.830* = 48 days and for *Msh2.1102* = 35 days (**** $p < 0.0001$), for *Ddit4.759* = 48 days (**** $p < 0.0001$) and *Ddit4.1432* = 56 days (** $p = 0.0028$) for *Cav1.351* = 38 and *Cav1.955* = 28 (**** $p < 0.0001$), for *Fancc.1512* = 59 days (** $p = 0.0083$), for *Polk.3595* = 53 days (* $p = 0.0122$) and for *Polk.1079* = 64 days ($p = \text{n.s.}$ (not significant)), for *Ercc5.1743* = 60 days (** $p = 0.0066$) and for *Ercc5.2801* = 73 days ($p = \text{n.s.}$), *Pms2.1907* = 73 days and *Pms2.535* = 129 days ($p = \text{n.s.}$), for *Mgmt.780* = 70 days and for *Mgmt.370* = 87 days ($p = \text{n.s.}$). p values shown indicate comparison to control. Survival curves for mice reconstituted with *Eμ-Myc* HSPCs transduced with a control shRNA vector (negative control) and those transduced with a *p53* shRNA (positive control) constitute the aggregate from several independent experiments and they are the same for all 9 panels shown and are also shown as controls in Figure 3b. **b** CIRCOS plots of log₂ fold-change in copy number (black dots) and intra-chromosomal structural variants (blue lines) in *Eμ-Myc* lymphomas accelerated by an shRNA against *p53* (#1162), *Cav1* (#1076), *Ddit4* (#1817), *Rnf144b* (#1790) and a control *Eμ-Myc* lymphoma (#1712) transduced with an shRNA targeting Renilla luciferase **c** Representative map illustrating mutations in *p53* and the indicated *p53* regulated-DNA damage repair genes in human colorectal cancers. Mutual exclusivity relative to mutations in *p53* was evaluated using cBioPortal tools (*** $p < 0.001$, ** $p < 0.001$, * $p < 0.01$). Full representation of the study is shown in Supplementary Fig. 20 a,b. **d** Model for *p53*-mediated tumour suppression.

Acknowledgements

We thank Drs S Lowe, A Lujambia, A Ventura and C Concepcion for the p53 target gene shRNA library and discussions; Drs M Ritchie, W Shi, Y Liao for data analysis, Drs JM Adams, P Bouillet, S Cory and A Villunger for gifts of mice and discussions. This work was supported by Postdoctoral Fellowships from the Leukemia & Lymphoma Society of America, Maria Curie Actions and Beatriu de Pinos, and Lady Tata Memorial Trust to A.J. and by grants from Cancer Australia and Cure Cancer Australia Foundation (grant no.1067571), the National Health and Medical Research Council (NHMRC; program grant no. 1016701, NHMRC Senior Principal Research Fellow [SPRF] Fellowship 1020363 to A.S.), and the Leukemia & Lymphoma Society of America (Specialized Center of Research [SCOR] grant no. 7001-13). This work was made possible by operational infrastructure grants through the Australian Government Independent Medical Research Institutes Infrastructure Support Scheme (IRIISS) and the Victorian State Government Operational Infrastructure Support (OIS).

Author Contributions The experiments were conceived and designed by AJ, MJH, LO'C and AS. Experiments were performed mainly by AJ with help from LJV, HY, LM, SW, CV, SM, AK, MSB, LML, RLS. Whole genome sequencing analysis was performed by LDS, MJW and ATP. The paper was written by AJ, MJH, LO'C and AS with help from the other authors.

Author Information The authors declare no competing financial interest. Correspondence and request of the material should be addressed to AS (strasser@wehi.edu.au).

References

- 1 Cheok, C. F., Verma, C. S., Baselga, J. & Lane, D. P. Translating p53 into the clinic. *Nat Rev Clin Oncol* **8**, 25-37, doi:10.1038/nrclinonc.2010.174 (2011).
- 2 Chan, T. A., Hwang, P. M., Hermeking, H., Kinzler, K. W. & Vogelstein, B. Cooperative effects of genes controlling the G₂/M checkpoint. *Genes Dev* **14**, 1584-1588 (2000).
- 3 Brady, C. A. *et al.* Distinct p53 transcriptional programs dictate acute DNA-damage responses and tumor suppression. *Cell* **145**, 571-583, doi:10.1016/j.cell.2011.03.035 (2011).
- 4 Li, T. *et al.* Tumor suppression in the absence of p53-mediated cell-cycle arrest, apoptosis, and senescence. *Cell* **149**, 1269-1283, doi:10.1016/j.cell.2012.04.026 (2012).
- 5 Valente, L. J. *et al.* p53 efficiently suppresses tumor development in the complete absence of its cell-cycle inhibitory and proapoptotic effectors p21, Puma, and Noxa. *Cell Rep* **3**, 1339-1345, doi:10.1016/j.celrep.2013.04.012 (2013).
- 6 Muller, P. A. & Vousden, K. H. p53 mutations in cancer. *Nat Cell Biol* **15**, 2-8, doi:10.1038/ncb2641 (2013).
- 7 Vogelstein, B., Lane, D. & Levine, A. J. Surfing the p53 network. *Nature* **408**, 307-310 (2000).
- 8 Lowe, S. W. *et al.* p53 status and the efficacy of cancer therapy *in vivo*. *Science* **266**, 807-810 (1994).
- 9 Donehower, L. A. *et al.* Mice deficient for p53 are developmentally normal but are susceptible to spontaneous tumours. *Nature* **356**, 215-221 (1992).
- 10 Jacks, T. *et al.* Tumor spectrum analysis in p53-mutant mice. *Curr Biol* **4**, 1-7 (1994).
- 11 Brady, C. A. & Attardi, L. D. p53 at a glance. *J Cell Sci* **123**, 2527-2532, doi:10.1242/jcs.064501 [pii]10.1242/jcs.064501 (2010).
- 12 Kenzelmann Broz, D. *et al.* Global genomic profiling reveals an extensive p53-regulated autophagy program contributing to key p53 responses. *Genes Dev* **27**, 1016-1031, doi:10.1101/gad.212282.112 (2013).
- 13 Jeffers, J. R. *et al.* Puma is an essential mediator of p53-dependent and -independent apoptotic pathways. *Cancer Cell* **4**, 321-328 (2003).
- 14 Villunger, A. *et al.* p53- and drug-induced apoptotic responses mediated by BH3-only proteins puma and noxa. *Science* **302**, 1036-1038, doi:10.1126/science.1090072 [pii] (2003).
- 15 Deng, C., Zhang, P., Harper, J. W., Elledge, S. J. & Leder, P. Mice lacking p21CIP1/WAF1 undergo normal development, but are defective in G1 checkpoint control. *Cell* **82**, 675-684 (1995).
- 16 Michalak, E. M. *et al.* Puma and to a lesser extent Noxa are suppressors of Myc-induced lymphomagenesis. *Cell Death Differ* **16**, 684-696 (2009).
- 17 Valente, L. J., Grabow, S., Vandenberg, C. J., Strasser, A. & Janic, A. Combined loss of PUMA and p21 accelerates c-MYC-driven lymphoma development considerably less than loss of one allele of p53. *Oncogene*, doi:10.1038/onc.2015.457 (2015).
- 18 Riley, T., Sontag, E., Chen, P. & Levine, A. Transcriptional control of human p53-regulated genes. *Nat Rev Mol Cell Biol* **9**, 402-412 (2008).
- 19 Lee, K., Tosti, E. & Edelmann, W. Mouse models of DNA mismatch repair in cancer research. *DNA Repair (Amst)* **38**, 140-146, doi:10.1016/j.dnarep.2015.11.015 (2016).

- 20 Zhu, H. *et al.* Involvement of Caveolin-1 in repair of DNA damage through both homologous recombination and non-homologous end joining. *PLoS ONE* **5**, e12055, doi:10.1371/journal.pone.0012055 (2010).
- 21 Razani, B. *et al.* Caveolin-1 null mice are viable but show evidence of hyperproliferative and vascular abnormalities. *J Biol Chem* **276**, 38121-38138, doi:10.1074/jbc.M105408200 (2001).
- 22 Bersani, C., Xu, L. D., Vilborg, A., Lui, W. O. & Wiman, K. G. Wig-1 regulates cell cycle arrest and cell death through the p53 targets FAS and 14-3-3sigma. *Oncogene* **33**, 4407-4417, doi:10.1038/onc.2013.594 (2014).
- 23 Harfe, B. D. & Jinks-Robertson, S. DNA mismatch repair and genetic instability. *Annu Rev Genet* **34**, 359-399, doi:10.1146/annurev.genet.34.1.359 (2000).
- 24 Malkin, D. *et al.* Germ line p53 mutations in a familial syndrome of breast cancer, sarcomas, and other neoplasms. *Science* **250**, 1233-1238 (1990).
- 25 Schneider, K., Zelley, K., Nichols, K. E. & Garber, J. *Li-Fraumeni Syndrome*, 1999 [updated 2013]).
- 26 Sengupta, S. & Harris, C. C. p53: traffic cop at the crossroads of DNA repair and recombination. *Nat Rev Mol Cell Biol* **6**, 44-55, doi:10.1038/nrm1546 (2005).
- 27 Lane, D. P. p53, guardian of the genome. *Nature* **358**, 15-16 (1992).
- 28 Dudgeon, C. *et al.* The evolution of thymic lymphomas in p53 knockout mice. *Genes Dev* **28**, 2613-2620, doi:10.1101/gad.252148.114 (2014).
- 29 Sofer, A., Lei, K., Johannessen, C. M. & Ellisen, L. W. Regulation of mTOR and cell growth in response to energy stress by REDD1. *Mol Cell Biol* **25**, 5834-5845, doi:10.1128/MCB.25.14.5834-5845.2005 (2005).
- 30 Williams, A. B. & Schumacher, B. p53 in the DNA-Damage-Repair Process. *Cold Spring Harb Perspect Med* **6**, doi:10.1101/cshperspect.a026070 (2016).

METHODS

Short hairpin RNA vectors. A miR-30-based shRNA library directed against p53 target genes was cloned into LMS (MSCV-based vectors)³¹ in pools of ~300 shRNAs, respectively. The genes that meet at least 3 of the 4 below listed p53 target criteria were included in the shRNA library directed towards p53 target genes: (1) presence of a p53 response element (RE) in the DNA close to or within the gene; (2) demonstration that the gene is either upregulated or downregulated at the mRNA and/or protein levels by the activated wild-type p53 protein (but not by mutant p53 protein); (3) evidence was derived by cloning the p53 RE from that gene, place it near a test gene, such as a luciferase reporter, and demonstrate that the wt p53 protein can regulate the test gene; (4) chromatin immunoprecipitation (CHIP) with a p53-specific antibody to demonstrate the presence of the p53 protein on the RE site in the DNA. Individual shRNAs for validation were synthesised as 97 bp oligos (Gene Works), PCR-amplified and cloned into LMS and LMP vectors³¹, which were verified by sequencing.

sgRNA lentiviral vectors. The constitutive sgRNA expression vectors were derived from the pFUGW vector, which has been described previously³², where the H1-sgRNA cassette has been inserted via Pac1 upstream of the UbiC Promoter and the eGFP cassette was replaced by a T2aCFP sequence (pFUT2aCFP). This vector was then linearised using Pac1, allowing the H1-*p53* or H1-*Mlh1* to be cloned into it. The sgRNA sequences are as follows: *p53*: 5'-GGCAACTATGGCTTCCACCT; *Mlh1*: 5'-AGCAGGAGTTATTCGGCGTC.

Lentiviral expression constructs for *Mlh1*. Whole gene synthesis was used to generate the *Mlh1* cDNA (Genscript). The cDNA corresponding to the full-length coding region of the MLH1 protein was flanked at the 5' end by a restriction site for EcoRI followed by a KOZAK and Flag sequence (5'-GAATTCACCATGGACTACAAGGACGACGATGACAAG-3') and the 3' end by a restriction site for BamH1. An *Mlh1*-Flag Δ NLS cDNA fragment encoding MLH1 with the nuclear localisation sequence (Δ NLS) deleted was generated as in⁴⁸. The cDNAs were cloned into the pFUT2aCFP vector that was linearised using Pac1, allowing the *p53* sgRNA to be cloned into it.

Retrovirus production and cell culture. Retroviral particles were produced by transient transfection of 293T cells grown in 10-cm Petri dishes with 10 μg of vector DNA along with the packaging retroviral constructs GAG (4.8 μg), and pENV (2.4 μg), and lentiviral constructs pMDL (5 μg), RSV (2.5 μg) and ENV (5 μg) using standard calcium phosphate precipitation as previously described³³. Virus containing supernatants were collected at 48-72 h after transfection and passed through a 0.45 μm filter. For infection of *E μ -Myc* lymphoma derived cell lines and WT MEF (mouse embryo fibroblast) lines, aliquots of 10^5 cells were suspended in 2 mL of virus-containing supernatant and then centrifuged at 2,200 rpm for 1.5 h at 32°C. Primary WT MEFs were prepared from E13.5 embryos. A single cell suspension of the body (excluding head and foetal liver) was prepared. All primary MEFs were used between passage 2 and 4. Primary WT MEFs were transformed with retroviruses expressing Ad5 E1A and H-Ras (G12V) onco-proteins as described above. The mouse 560 *E μ -Myc* lymphoma cell line was cultured in high-glucose DMEM supplemented with 10% heat-inactivated FCS, 50 μM β -mercaptoethanol (Sigma), 100 μM asparagine (Sigma), 100 U/mL penicillin and 100 mg/mL streptomycin in a humidified incubator at 37°C, 10% CO₂.

Cell viability assays. Thymi and bone marrow were harvested from mice of the indicated genotypes and single cell suspensions prepared. Cells were cultured in high-glucose DMEM supplemented with 10% heat-inactivated FCS, 50 μM β -mercaptoethanol (Sigma), 100 μM asparagine (Sigma), 100 U/mL penicillin and 100 mg/mL streptomycin in a humidified incubator at 37°C, 10% CO₂. Cells were plated into 96-well flat-bottom plates at a starting density of 5×10^4 cells/well and treated with the indicated stimuli, as described³⁴. Cell viability was determined by staining with propidium iodide (PI) plus FITC-conjugate Annexin V followed by flow cytometric analysis on a BD-Biosciences LSRW flow cytometer with 10,000 cells recorded per sample. Data were analysed using FlowJo analysis software.

Cell cycle analysis. Spleens were harvested from mice of the indicated genotypes and single-cell suspensions were prepared. Cells were plated at 5×10^4 cells/well into 96-well plates, in triplicate for each treatment, coated with 1 $\mu\text{g}/\text{mL}$ anti-CD40 (FGK45) plus 10 $\mu\text{g}/\text{mL}$ anti-IgM F(ab')₂ antibody fragments (Jackson ImmunoResearch) and incubated for 96 h in high-glucose RPMI-1640 media supplemented with 10% heat-inactivated FCS, 50 μM β -mercaptoethanol (Sigma),

100 μ M asparagine (Sigma), 10mM HEPES, 2mM glutamine, 0.1mM non-essential amino acids, 1mM sodium-pyruvate, and 100 U/mL penicillin and 100 mg/mL streptomycin in a humidified incubator at 37°C, 10% CO₂. To track cell division, cells were labeled with 5 μ M CellTrace Violet (CTV) (Life Technologies) at 5 μ M, according to the manufacturer's instructions. CTV dilution was assessed by flow cytometry, gating first on live B cells (B220⁺ and PI⁻). Flow cytometric analysis was performed on a BD-Biosciences LSR IIW flow cytometer. Data were analyzed using FlowJo software (Treestar). Bone marrow was harvested from mice of the indicated genotypes and single-cell suspensions were prepared. Cells were plated at 5 x 10⁵ cells/well into 96-well flat-bottom plates, fixed, permeabilised and stained with DAPI for flow cytometric cell-cycle analysis using a BD-Biosciences LSR IIW flow cytometer. Data were analysed using FlowJo analysis software (Tree Star) and distribution of cells within the distinct stages of the cell cycle determined by applying the Watson (pragmatic) cell-cycle modeling algorithm to the DAPI fluorescence intensity profile of the cells.

Senescence-associated β -galactosidase activity assay. WT, *p53*^{-/-} and *Zmat3*^{-/-} MEFs were prepared from E13.5 embryos. A single cell suspension of the body (excluding head and foetal liver) was prepared. MEFs between passage 6 and 7 were fixed in 2% formaldehyde 0.2% glutaraldehyde and incubated with X-gal (Invitrogen) at pH 6.0 for 14 h to determine senescence associated β -galactosidase activity, as previously described³⁵.

Animal experiments. Experiments with mice were conducted according to the guidelines of The Walter and Eliza Hall Institute animal ethics committee. *E μ -Myc*, *E μ -Myc;Puma*^{-/-}16, *Puma*^{-/-}; *p21*^{-/-} and *p53*^{-/-}10 mice were all maintained on a C57BL/6-Ly5.2+ background. The CAS9 mice were on a C57BL/6-Ly5.2 background (Fig. 3e) and on a mixed C57BL6/129SV background (Supplementary Fig. 13b) For haematopoietic reconstitution, fresh embryonic day 13.5 (E13.5) foetal liver cells (a rich source of HSPCs) were obtained and placed into alpha-minimum essential medium (α -MEM) with glutamax (Gibco) supplemented with 10% FCS (foetal calf serum; Gibco), 1 mM L-glutamine, 1 mM sodium pyruvate, 100 μ g/mL streptomycin, 100 U/mL penicillin, 10 mM HEPES, 50 μ M β -mercaptoethanol containing the cytokines IL-6 (10 ng/mL), stem cell factor (100 ng/mL), thrombopoietin (50 ng/mL) and FLT-3 ligand (10 ng/mL). Foetal liver cells were maintained in culture for approximately 48 h for retroviral/lentiviral infection. Viral supernatants

were collected as described above. Infections were performed in a 6-well non-tissue-culture-treated plate that had been coated overnight with retronectin solution (32 $\mu\text{g}/\text{mL}$ in PBS) at 4°C followed by coating with 2% albumin solution from bovine serum (Sigma-Aldrich A1595) in PBS at 37°C for 30 min prior to coating with viral particles. Viral particles were centrifuged onto the retronectin-coated plates at 3,000 rpm for 1 h. Foetal liver cells were then added to each well and incubated for 24 h. HSPCs transduced with vectors encoding shRNAs or sgRNAs were collected, washed in PBS, and injected into lethally irradiated (2x5.5 Gy, 4 h apart) C57BL/6-Ly5.1+ mice. *E μ -Myc;Cas9* HSPCs transduced with sgRNAs were collected, washed in PBS and then injected into sub-lethally irradiated (2.5 Gy) Rag1^{tm1Mom}/J mice (Supplementary Fig. 13b). Reconstituted animals were monitored for illness by lymph node/spleen palpation and overall appearance. Survival time was defined as the time from haematopoietic reconstitution until the animal became ill and had to be sacrificed for ethical reasons.

Generation of *Zmat3*-deficient mice. CRISPR/CAS9 mediated generation of *Zmat3* mutant mice was performed as previously described^{36,37}. *Cas9* mRNA (20 ng/ μL) and sgRNAs (10 ng/ μL) of the sequence sgRNA#1 GTCAAGCATACTCCATACCC and sgRNA#2 GCGGTGTGAATTGCTGTGCC were injected into the cytoplasm of fertilized one-cell stage embryos. 19,772 bp of genomic sequence spanning exons 2 to 5 was targeted for deletion. After 24 h, two-cell stage embryos were transferred into the uteri of pseudo-pregnant female C57BL/6J mice. Viable offspring were genotyped by next-generation sequencing as previously described³².

shRNA recovery, identification and determination of representation. Genomic DNA was isolated from tumour cells using PureLink® Genomic DNA (ThermoFisher) and amplified the integrated shRNAs using PCR, and sequenced the amplified products on Illumina MiSeq. For identifying the shRNAs and to determine their representation, the sequence reads were aligned to a list of all shRNAs used in the screen.

Illumina MiSeq sequencing. Each dual indexed library plate pool was quantified using the Agilent Tape station and the Qubit RNA assay kit for Qubit 2.0 Fluorometer (Life Technologies). The indexed pool was diluted to 12 pM for sequencing on a MiSeq instrument (Illumina) according to the manufacturer's instructions. The 300-cycle kit was used for amplicon sizes of less than 280

bp, and these amplicons were sequenced as single reads (281 cycles) followed by a 44-cycle second index read. Amplicons that were larger than 280 bp were sequenced using the 600-cycle kit, and both reads 1 and 2 were sequenced for 311 cycles.

Library preparation and whole genome sequencing. An input of 100 ng of genomic DNA per lymphoma or pre-leukaemic cell (#1400, #1401, #1497, #1420, #1494, #1314, #1649, #1651) was prepared and indexed for Illumina sequencing using the TruSeq DNA sample Prep Kit (Illumina) according to the manufacturer's instruction. The library was quantified using the Agilent TapeStation and the Qubit™ RNA assay kit for Qubit 3.0® Fluorometer (Life Technologies). The indexed libraries were then pooled and prepared for paired end sequencing on a NextSeq500 instrument using the 150-cycle kit v2 chemistry (Illumina) as per manufacturer's instructions. A total of 10 NextSeq runs were completed which generated 4 billion 2x 75 base paired end reads for subsequent analysis. The base calling and quality scoring were determined using Real-Time Analysis on board software v2.4.6, while the FASTQ file generation and de-multiplexing utilised bcl2fastq conversion software v2.15.0.4. Whole genome sequencing libraries for lymphomas and pre-leukaemic cell samples (#1620, #1076, #1085, #1817, #1818, #1162, #1712, #1790, #1791) were prepared using the TruSeq Nano DNA Library Preparation Kit (Illumina, San Diego) and sequenced to an average depth of 30x at Genome One (Garvan Institute, Sydney) on the Illumina HiSeq X Ten platform.

Whole genome sequence analysis. Sequencing reads were aligned to the GRCm38/mm10 reference genome using bwa mem (version 0.7.15-r1140)³⁸ with default settings. *Single nucleotide variants.* We called single nucleotide variants (SNVs) using multiSNV version 2.3³⁹ with default settings, treating sample #1649 (derived from pre-leukaemic, non-infected *Eμ-Myc* B lymphoid cells) as the “normal” and the remaining seven samples as “lymphomas”. We ignored calls with a double-reference genotype, or with a quality score less than 90. Loci were excluded from consideration wherever multiSNV either called more than one non-reference allele, or tagged an allele with filters other than “PASS”. We also excluded those loci with called changes in more than one of the six lymphoma samples. We then applied a number of quality control filters: loci were excluded from consideration if they overlapped regions in the mm10 blacklist produced by the ENCODE project [<https://www.encodeproject.org/files/ENCFF547ME>]; if they coincided

with the coordinates of SNPs in dbSNP142

[<http://hgdownload.soe.ucsc.edu/goldenPath/mm10/database/snp142.txt.gz>]; if they occurred in repeats annotated by RepeatMasker

[<http://hgdownload.cse.ucsc.edu/goldenPath/mm10/database/rmsk.txt.gz>]; or if they occurred in regions of 100mer mappability less than 1, computed for mm10 using the GEM software suite⁴⁰ SNVs were annotated with their flanking bases using functions from the software package VariantAnnotation⁴¹. This approach detects substitutions that occur in the population at a SNV frequency of more than approximately 5%, and will have an increasing false negative rate as population diversity increases. Substitution rate analysis was therefore restricted to malignant lymphoma samples where clonal selection minimises this effect.

Short tandem repeat (STR) genotyping. We called STR genotypes using HipSTR version v0.4⁴², filtering using the included “filter_vcf.py” script. We included in our analysis those genotypes that were called with a posterior probability of >0.9 (unphased) and in which there was at least a 1 base-pair difference from the mm10 reference genome. We excluded sites where all eight samples had the same genotype (even where this was distinct from the reference genotype). For STR genotyping, samples #1649, #1651, #1314, #1420, #1497, #1494, #1400 and #1401 were processed separately to samples #1620, #1818, #1817, #1791, #1790, #1712, #1162, #1085 and #1076.

Copy number and structural variant calling. Smoothed copy number estimates were produced by qnaseq⁴³ with a 100 kb bin size, excluding from considerations regions in the mm10 ENCODE blacklist [<https://www.encodeproject.org/files/ENCFF547ME>]. We called structural variants using GRIDSS version 1.3.4⁴⁴ with default settings, excluding those sites not marked “PASS” and applying region-based filtering similar to that we applied to SNV calls: loci were excluded from consideration if they overlapped regions in the ENCODE mm10 blacklist [<https://www.encodeproject.org/files/ENCFF547ME>]; if they coincided with the coordinates of deletions or in-dels in dbSNP142

[<http://hgdownload.soe.ucsc.edu/goldenPath/mm10/database/snp142.txt.gz>]; if they occurred in repeats annotated by RepeatMasker

[<http://hgdownload.cse.ucsc.edu/goldenPath/mm10/database/rmsk.txt.gz>]; or if they occurred in regions of 100mer mappability less than 1⁴⁵. Structural variants were included if they had a QUAL score of greater than 500 in one sample and 0 in the remaining samples. CIRCOS-style plots were

produced with the software package `ggbio`⁴⁶. } For copy number analysis and variant calling, samples #1649, #1651, #1314, #1420, #1497, #1494, #1400 and #1401 were processed separately to samples #1620, #1818, #1817, #1791, #1790, #1712, #1162, #1085 and #1076.

Analysis of mutual exclusivity of mutations in different genes in human cancers. Mutual exclusivity between mutations in *p53* and mutations in *p53* activated DNA damage repair genes was evaluated in human colorectal and haematological cancers. Mutual exclusivity plots were generated using the online cBioPortal tools (cbioportal.org). P values were calculated using the Fisher exact test.

Flow cytometric analysis and cell sorting. Assessment of eGFP in tumour cells and immunophenotyping of lymphomas and leukaemias were performed using LSR IIW or FACS Calibur flow cytometers (Becton Dickinson). Immunophenotyping of lymphomas and leukaemias was performed on single-cell suspensions that had been stained with surface-marker-specific antibodies. The following fluorochrome-conjugated antibodies were utilised: B220 (RA3-6B2), IgM (5.1), IgD (11-26C), CD4 (H129), CD8 (YTS.169), MAC-1 (M1/70), and GR-1 (RB6-8C5). To confirm that the lymphomas or leukaemias were of donor haematopoietic cell derived origin, staining for Ly5.2 (5.405.15.2) was performed, in addition to verifying that they were GFP⁺. Antibodies were produced in our laboratory and conjugated to R-phycoerythrin (R-PE) or allophycocyanin according to the manufacturer's (Prozyme) instructions. Virally transduced cell lines were sorted using Aria W (Becton Dickinson) by enriching for eGFP-positive cells.

Western blot analysis. Total protein extracts were prepared from primary MEF lines, *Eμ-Myc* lymphoma cell lines, primary lymphomas and bone marrow derived pre-leukaemic B lymphoid cells by lysis in RIPA buffer supplemented with protease inhibitors (complete protease inhibitor cocktail, Roche). Protein content in extracts was quantitated using the Bradford assay (Bio-Rad). Protein were separated by SDS-PAGE (ThermoFisher) and transferred onto nitrocellulose membranes (ThermoFisher). Membranes were blocked using 5% milk in PBS with 0.1% Tween 20 prior to incubation with the primary antibody. Polyclonal antibodies were used to detect mouse ZMAT3 (Sigma-Aldrich, AV50793), p53 (Novocastra, Leica, CM5) and MLH1 (Calbiochem, PC56). Monoclonal antibodies were used to detect mouse CAV1 (BD Biosciences, 610406) and

HSP70 (clone N6; a gift from Dr Robin Andersson, Olivia Newton John Cancer Centre, Heidelberg, VIC, Australia). For checking mTOR activity, *Eμ-Myc* lymphoma cells were lysed in 20 mM Tris pH 7.5, 135 mM NaCl, 1.5 mM EDTA, 10% glycerol, 1% Triton X-100 including protease inhibitors (Roche, Dee Why, NSW, Australia). Equal amounts of protein were separated on 10% NUPAGE® Bis Tris gels (Invitrogen), transferred to PVDF, and blotted with the following antibodies from Cell Signalling: LC3B (D11), p-ULK1^{S757} (D7O6U), ULK1 (D8H5), p-S6^{S240/244} (D68F8), S6 (5G10), p-4E-BP1^{S65} (#9451), 4E-BP1 (53H11), and SQSTM1 (#5114). The antibody against β-actin (loading control) was purchased from Sigma (AC-15).

DNA damage repair analysis (comet assay). The single-cell gel electrophoresis (Comet assay) was used to measure DNA damage in pre-leukaemic *Eμ-Myc* and *Eμ-Myc;Puma*^{-/-} bone marrow derived B lymphoid cells. Bone marrow cells were harvested from the femora of pre-leukaemic mice at 10-12 days after reconstitution. Donor derived, transduced B lymphoid cells (B220⁺GFP⁺) were purified by FACS sorting and the comet assay was performed according to the manufacturer's instructions (The Trevigen CometAssay #4250-050-K). The slides were analysed at 10x magnification under a Nikon 90i microscope for pre-leukaemic *Eμ-Myc;Puma*^{-/-} B lymphoid cells (Supplementary Fig. 7a,b) and under a Nikon TiE Live Cell Imaging microscope for pre-leukaemic *Eμ-Myc* B lymphoid cells (Supplementary Fig. 11b). The comet tail moment was measured by blinded scoring of the images using the Matamorph image analysis software.

qRT-PCR analysis. Total RNA was isolated from FACS sorted lymphoma cells, thymocytes or E1A/H-Ras transformed MEFs using TRIzol® (ThermoFisher) and reverse transcribed using SuperScript II Reverse Transcriptase (ThermoFisher) and Oligo-d(T) primers. qRT-PCR was performed in triplicate using Taqman® Gene Expression assays (ThermoFisher) and an ABI 7900 and ViiA7 Real-time PCR machine. The mRNA expression levels of p53 target genes of interest were standardised by the transcript levels of the reference gene, *Hmbs*, based on the comparative threshold method ($\Delta\Delta C_t$).

Statistical analysis. Prism (Version 7; GraphPad Software) software was used for all statistical analyses. Two-group comparisons were made using 2-tailed *t* tests assuming equal variances. Tumor free survival data were plotted using Kaplan-Meier curves. Differences in survival time

between cohorts of mice were tested using log-rank tests. *P* values less than 0.05 were considered to indicate statistical significance.

References:

- 31 Dickins, R. A. *et al.* Probing tumor phenotypes using stable and regulated synthetic microRNA precursors. *Nat Genet* **37**, 1289-1295 (2005).
- 32 Aubrey, B. J. *et al.* An Inducible Lentiviral Guide RNA Platform Enables the Identification of Tumor-Essential Genes and Tumor-Promoting Mutations In Vivo. *Cell Rep* **10**, 1422-1432, doi:10.1016/j.celrep.2015.02.002 (2015).
- 33 Lois, C., Hong, E. J., Pease, S., Brown, E. J. & Baltimore, D. Germline transmission and tissue-specific expression of transgenes delivered by lentiviral vectors. *Science* **295**, 868-872, doi:10.1126/science.1067081 [pii] (2002).
- 34 Herold, M. J., van den Brandt, J., Seibler, J. & Reichardt, H. M. Inducible and reversible gene silencing by stable integration of an shRNA-encoding lentivirus in transgenic rats. *Proc Natl Acad Sci U S A* **105**, 18507-18512, doi:10.1073/pnas.0806213105 (2008).
- 35 Strasser, A. *et al.* Enforced *BCL2* expression in B-lymphoid cells prolongs antibody responses and elicits autoimmune disease. *Proc Natl Acad Sci U S A* **88**, 8661-8665 (1991).
- 36 Dimri, G. P. *et al.* A biomarker that identifies senescent human cells in culture and in aging skin in vivo. *Proc Natl Acad Sci U S A* **92**, 9363-9367 (1995).
- 37 Wang, H. *et al.* One-step generation of mice carrying mutations in multiple genes by CRISPR/Cas-mediated genome engineering. *Cell* **153**, 910-918, doi:10.1016/j.cell.2013.04.025 (2013).
- 38 Kueh, A. J. *et al.* An update on using CRISPR/Cas9 in the one-cell stage mouse embryo for generating complex mutant alleles. *Cell Death Differ* **24**, 1821-1822, doi:10.1038/cdd.2017.122 (2017).
- 39 Li, H. Aligning sequence reads, clone sequences and assembly contigs with BWA-MEM. *arXiv:1303.3997 [q-bio]* (2013).
- 40 Josephidou, M., Lynch, A. G. & Tavaré, S. multiSNV: a probabilistic approach for improving detection of somatic point mutations from multiple related tumour samples. *Nucleic Acids Research* **43**, e61-e61, doi:10.1093/nar/gkv135 (2015).
- 41 Derrien, T. *et al.* Fast Computation and Applications of Genome Mappability. *PLoS ONE* **7**, e30377, doi:10.1371/journal.pone.0030377 (2012).
- 42 Obenchain, V. *et al.* VariantAnnotation : a Bioconductor package for exploration and annotation of genetic variants. *Bioinformatics* **30**, 2076-2078, doi:10.1093/bioinformatics/btu168 (2014).
- 43 Willems, T. *et al.* Genome-wide profiling of heritable and de novo STR variations. *Nat Meth* **14**, 590-592, doi:10.1038/nmeth.4267 (2017).
- 44 Scheinin, I. *et al.* DNA copy number analysis of fresh and formalin-fixed specimens by shallow whole-genome sequencing with identification and exclusion of problematic regions in the genome assembly. *Genome Res.* **24**, 2022-2032, doi:10.1101/gr.175141.114 (2014).
- 45 Cameron, D. L. *et al.* GRIDSS: sensitive and specific genomic rearrangement detection using positional de Bruijn graph assembly. *bioRxiv*, 110387, doi:10.1101/110387 (2017).
- 46 Cameron, D. L. *et al.* GRIDSS: sensitive and specific genomic rearrangement detection using positional de Bruijn graph assembly. *Genome Res* **27**, 2050-2060, doi:10.1101/gr.222109.117 (2017).
- 47 Yin, T., Cook, D. & Lawrence, M. ggbio: an R package for extending the grammar of graphics for genomic data. *Genome Biol* **13**, R77, doi:10.1186/gb-2012-13-8-r77 (2012).

- 48 Wu, X. *et al.* Dimerization of MLH1 and PMS2 limits nuclear localization of MutL. *Molecular and Cellular Biology* **23**, 3320-3328, doi:10.1128/MCB.23.9.3320-3328 (2003)]